Robust Automotive Suspension Design Using Adaptive Response Surface Based Multi-Objective Optimization

Paul Tobe Ubben[1*], Jürgen Haug[1], Dieter Bestle[2]

[1] Daimler AG - Group Research & Advanced Engineering, Sindelfingen, Germany

[2] BTU - Engineering Mechanics and Vehicle Dynamics, Cottbus, Germany

Abstract

Deterministic optimization is used in all fields of engineering, especially in early design processes based on digital prototypes and simulation. A major disadvantage of deterministic optimization is the unknown robustness of the found solution against uncertainties of system parameters. Therefore, the Robust Design Optimization (RDO) concept as combination of Robustness Analysis (RA) and deterministic optimization was developed. In this paper, such an approach is applied to the optimization of a suspension for passenger cars w.r.t. typical driving maneuvers. The suspension behavior has to be robust against uncertainties without defining strict limits or safety margins. The coupled multi-objective RDO procedure will find a Pareto-front w.r.t. mean value and variance of chosen objectives. As a result, a specific compromise regarding system robustness and mean performance may be chosen from this Pareto-set. To overcome the vast amount of CPU-time, required for expensive direct function evaluations, an adaptive response surface method (aRSM) is integrated. The overall process then consists of an inner loop involving a multi-objective evolutionary algorithm based on response surfaces and an outer loop, where metamodeling is performed on a set of support points. This set is initialized in the first iteration step and updated afterwards by picking promising designs from the Pareto-fronts of the surrogate model, which are then evaluated exactly.

Keywords: Multi-objective optimization, Robust design, Adaptive response surface, Suspension design

[*] Kontakt: Dipl.-Ing. Paul Tobe Ubben, Daimler AG, HPC X578, 71059 Sindelfingen, Germany, paul_tobe.ubben@daimler.com

1 Introduction

Since decades, automotive experts have gained a profound level of knowledge in the field of conventional suspension design leading to a high degree of maturity of current car suspensions. To realize further improvements, it is inevitable to increase complexity by introducing more sophisticated designs. In parallel, the needs with respect to robustness are dramatically increasing due to a still growing number of derivatives on the one hand and a wider spectrum of wheel load variations by introducing electric batteries for plug-in and pure electrically driven cars on the other hand. Under these circumstances, optimal solutions are hard to find by human search. Computer-based optimization used in the digital phase of suspension development may help to improve insight into the system and to realize better designs.

In literature most publications are related to deterministic optimization of vehicle suspensions, whereas RDO is seldomly used yet. Most RDO procedures are based on response surface modeling (RSM) applied in different ways to cut down evaluation effort. In cases where only design parameters are scattering, it may be appropriate to build up a global metamodel. Design objectives can then be evaluated based upon the metamodel, and especially the time-consuming determination of robustness measures can be speeded up remarkably. Nevertheless, excellent approximation quality is necessary to obtain trustworthy results as discussed by Most and Will [1]. Cheng and Lin [2] use such a non-adaptive global metamodel for multi-objective robust suspension design w.r.t. joint position and manufacturing errors of joint positions. Objectives are mean value and variance of characteristic suspension specific values. The metamodel is based on an initial sample obtained by a Design of Experiments (DOE) method. Kang et al. [3] and Park et al. [4] added an adaptive strategy. The objective's mean values and standard deviations are weighted and summed up in order to get a single-objective RDO. Optimization is performed on the metamodel, and the found optimal design is originally evaluated and added to the set of sample points for updating the metamodel. This procedure is repeated until a convergence criterion is fulfilled or a maximum number of iterations is reached. Yang et al. [5] use a similar approach where a so called dual-response surface method is chosen to approximate mean value and variance separately. Another way to profit from metamodels is to use them just as local approximations to improve evaluation of robustness measures as presented by Busch and Bestle [6]. For each deterministic design, a sample of uncertain parameters is generated and a metamodel is built up. Based on this model, robustness analysis is performed with a huge number of samples. The number of costly direct function evaluations is reduced dramatically and it could be shown that the estimation quality of mean value and variance even increases.

The mentioned investigations focus on optimizing a single car in the presence of uncertainties such as customer loading or manufacturing tolerances. Besides optimizing individual car suspensions, however, it is also desirable to ensure consistent ride and handling behavior for a whole car segment including different engines, extra equipment, plug-in batteries and

customer loading. Thus, a suspension should be designed such that it can be used in several derivatives such as sedans, station wagons, coupes, etc. This may be achieved by using RDO as will be shown by an approach based on optiSLang [7].
This paper is organized as follows: In Section 2, a brief overview of different RDO approaches is given. A specific RDO process is chosen and explained in detail in Section 3, where its functionality is shown by application to a test function. In chapter 4 the developed process is adapted for designing a car suspension for a given set of design parameters and uncertainties. Finally, the results of the proposed RDO process are summarized and a conclusion is given.

2 Robust Design Optimization

Generally, RDO is an optimization performed under consideration of uncertainties. Typical tasks are to optimize a given objective while fulfilling constraints with a specified safety margin or minimizing the variance of the objective with respect to uncertainties. RDO can be divided into stochastic design optimization and fuzzy logic, where the present work focuses on stochastic design optimization consisting of variance-based analysis and probability-based analysis [8]. The selection of one of these techniques depends on the specific area of application. Probability-based analysis is recommended for system design where a specific and very low failure probability is needed. Variance-based analysis can be used to prove safety margins up to three sigma with an affordable number of samples [1]. This paper focuses on variance-based methods. Therefore, subsequently speaking of RDO refers to this kind of RDO technique.
In literature two general variance-based RDO procedures can be found: an integrated approach, also known as coupled procedure, and an iterative approach [1][9]. In the following, both strategies will be discussed and reasons for the selection w.r.t. the specific field of application will be given.
Iterative RDO firstly performs a deterministic optimization without taking robustness measures into account, and robustness evaluation is only done afterwards. In this procedure robustness is usually considered by introducing safety factors which need to be fulfilled. If a deterministic optimum is infeasible by violating one of the predefined robustness dependent constraints, safety factors are updated in order to get a feasible optimum in the next iteration step. This is repeated until a maximum number of iterations is reached or a convergence criterion is fulfilled. Figure 1a shows a flowchart of the procedure. The benefit of this iterative process is that robustness analysis is performed only once in each outer iteration loop, namely for the deterministic optima. The main drawback is, however, that it is impossible to achieve a robust design in terms of minimizing robustness measures, e.g. response variances.
If robustness measures are used during optimization already, the procedure is considered as integrated RDO. For each design generated by the optimization algorithm a robustness evaluation is performed according to Figure 1b. Hence, the possibility of taking robustness

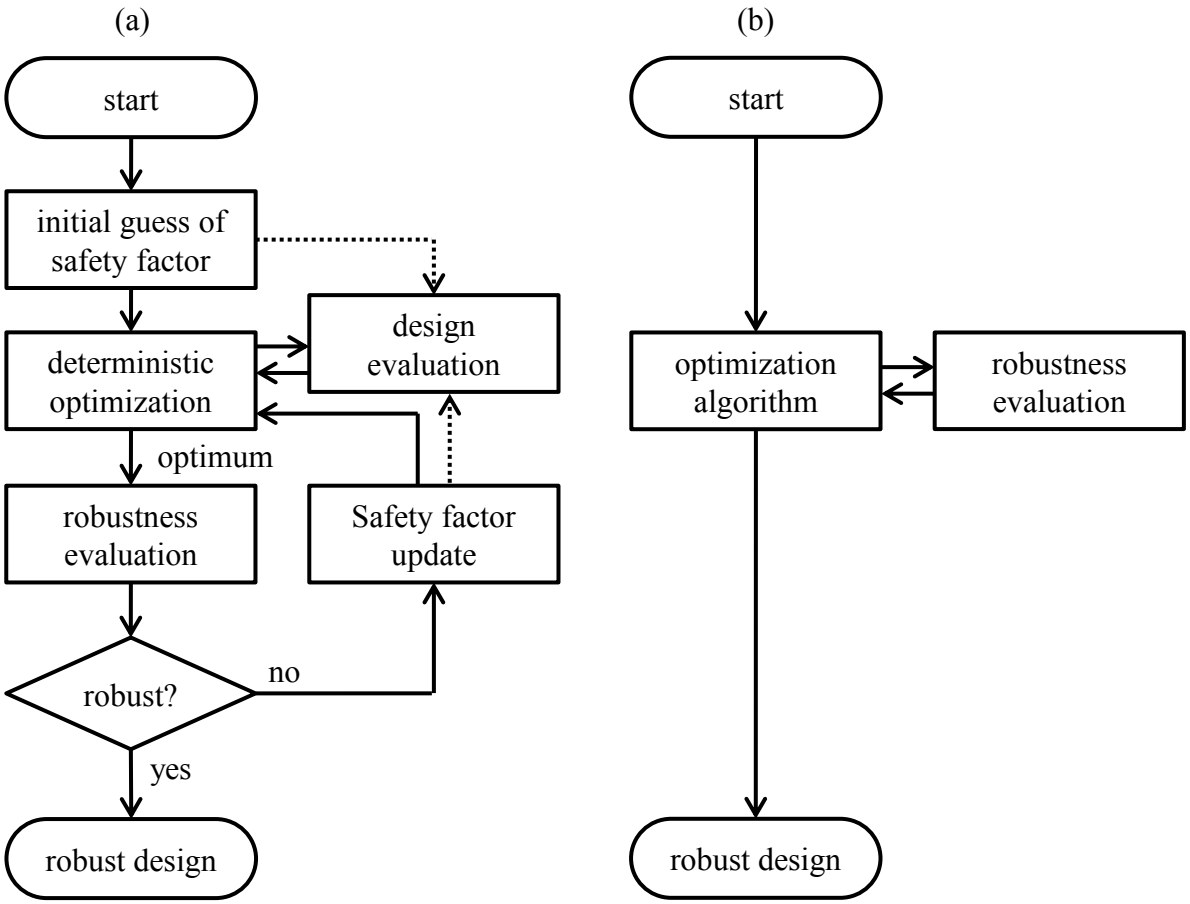

Figure 1: Iterative (a) and integrated (b) RDO procedure

constraints into account while optimizing response variances and mean values is given. Besides having more options to set up the RDO task, this procedure needs a vast amount of CPU-time for expensive direct function evaluations. Hence, an efficient design evaluation process is needed if time-consuming simulations are involved.
In the present work robustness is required in terms of minimizing the variance of model responses without having constraints such as strict safety margins. Therefore, the integrated RDO procedure is chosen, although more effort has to be spend on cutting down the number of direct function evaluations.

3 Adaptive Response Surface Based RDO

As mentioned above, RSM is an opportunity to minimize the amount of CPU-time needed for the RDO process. Here, an adaptive response surface (aRS) based multi-objective RDO is used and explained in the following.

3.1 Extended Problem Formulation

The goal is to optimize a system in terms of minimizing mean and standard deviation of an objective function $f(\boldsymbol{p};\boldsymbol{r})$ with a given set of h design parameters p_i summarized in design vector $\boldsymbol{p}$ between some bounds $\boldsymbol{p}_l$, $\boldsymbol{p}_u$ and with normally distributed stochastic variables $\boldsymbol{r}\sim N(\boldsymbol{\mu}_r, \boldsymbol{\Sigma}_r)$ with mean $\boldsymbol{\mu}_r$ and covariance matrix $\boldsymbol{\Sigma}_r$ representing uncertainties. Hence, the RDO problem may be formulated as

$$\min_{\boldsymbol{p}\in P} f(\boldsymbol{p};\boldsymbol{r}) \; s.t. \; P = \{\boldsymbol{p} \in \mathbb{R}^h | \boldsymbol{p}_l \leq \boldsymbol{p} \leq \boldsymbol{p}_u\}. \tag{1}$$

Here the integrated RDO procedure described above is used where the stochastic variables $\boldsymbol{r}$ are eliminated by searching simultaneously for good mean performance $\mu_f(\boldsymbol{p}) = E[f(\boldsymbol{p};\boldsymbol{r})]$ and low scatter $\sigma_f(\boldsymbol{p}) = \sqrt{E\left[\left(f(\boldsymbol{p};\boldsymbol{r}) - \mu_f\right)^2\right]}$. This yields a bi-criterion problem

$$\min_{\boldsymbol{p}\in P} \boldsymbol{f}^{RDO}(\boldsymbol{p}) \; s.t. \; P = \{\boldsymbol{p} \in \mathbb{R}^h | \boldsymbol{p}_l \leq \boldsymbol{p} \leq \boldsymbol{p}_u\} \tag{2}$$

where

$$\boldsymbol{f}^{RDO}(\boldsymbol{p}) \coloneqq \begin{bmatrix}\mu_f \\ \sigma_f\end{bmatrix}. \tag{3}$$

The solution process consists of two parts: An initial sampling and the main RDO loop consisting of different process steps, see Figure 2. In the first part a predefined number of sample designs $\boldsymbol{p}_j$ are generated. To avoid purely distributed inputs, particularly for a small amount of samples, advanced Latin Hypercube Sampling (aLHS) [10] is used supplemented by a single-switch-optimized method for reducing correlation errors. The resulting set of sample points acts as set of support points

$$S^{(i)} = \left\{\boldsymbol{p}_j, j = 1 \ldots J^{(i)}\right\} \tag{4}$$

for generating response surfaces , where $i = 0$ for the initial set.

In the first step of the main RDO loop, response surfaces $\hat{\boldsymbol{f}}^{RDO}(\boldsymbol{p}) = \boldsymbol{f}^{RDO}(\boldsymbol{p}) + \boldsymbol{\varepsilon}(\boldsymbol{p})$ are built up from the actual set of support points $\boldsymbol{p}_j \in S^{(i)}$ and associated function values $\boldsymbol{f}_j^{RDO} = \boldsymbol{f}^{RDO}(\boldsymbol{p}_j)$. Estimation of $\boldsymbol{f}^{RDO}(\boldsymbol{p}_j)$ according to Equation (3) requires a sample for the stochastic variables $\boldsymbol{r}$ which is generated in the same way as initial designs $\boldsymbol{p}_j \in S^{(0)}$ by using aLHS, but based on a predefined probability density function.

For approximation purpose the metamodel of optimized prognosis (MoP) is used [11]. Briefly said, MoP is an automatic approach which searches for the best response surface technique for a given dataset with respect to a specific validation method. Currently polynomial least squares approximation, moving least squares and ordinary Kriging are implemented in optiSLang [12].

After generating the metamodels, the optimization problem (2) is solved on the response surfaces:

$$\min_{\boldsymbol{p}\in P} \hat{\boldsymbol{f}}^{RDO}(\boldsymbol{p}) \text{ s.t. } P = \{\boldsymbol{p} \in \mathbb{R}^h | \boldsymbol{p}_l \leq \boldsymbol{p} \leq \boldsymbol{p}_u\}. \quad (5)$$

A global evolutionary optimization algorithm based on the Strength Pareto Evolutionary Algorithm (SPEA2) [13] is used. The algorithm generates a Pareto-front of optimal compromises between low mean value μ_f and low scatter σ_f dominating the remaining designs. The algorithm finishes if a predefined number of iterations is reached or the archive

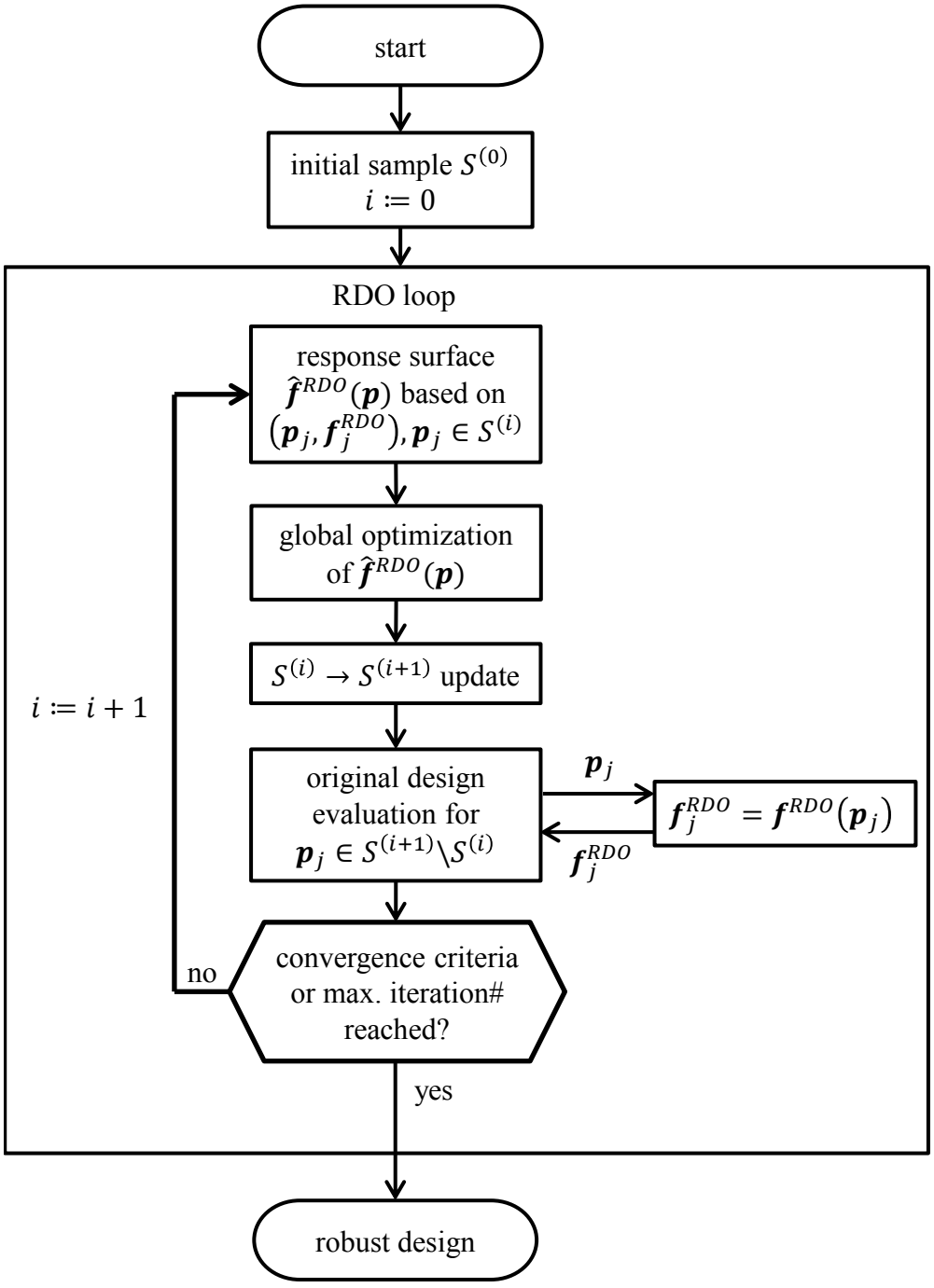

Figure 2: aRS based RDO process

of non-dominated individuals stagnates. The result of the optimization is a set of non-dominated compromise designs $\mathcal{C} = \{\boldsymbol{p}_k^P, k = 1 \dots K\}$ and a remaining set of dominated designs $\mathcal{D} = \{\boldsymbol{p}_k^D, k = 1 \dots \overline{K}\}$ which is usually of no interest, but may be used here as explained later.

In the next step, proper sample points for the adaption of the response surfaces have to be selected, which is done according to Figure 3. At first, minimum distances between non-dominated designs $\boldsymbol{p}_k \in \mathcal{C}$ and all points of actual set $S^{(i+1)} := S^{(i)}$ are calculated:

$$d(\boldsymbol{p}_k) := dist\left(\boldsymbol{p}_k, S^{(i+1)}\right) := \min_{\boldsymbol{p}_j \in S^{(i+1)}} \left\|\boldsymbol{p}_k - \boldsymbol{p}_j\right\|. \tag{6}$$

The design $\boldsymbol{p}_{k^*}$ with the maximum distance $d(\boldsymbol{p}_{k^*})$ is then chosen as a new potential RS support point and removed from the set of non-dominated designs $\mathcal{C}$. In order to prevent selection of new support points lying too close to others or being even identical to an already existing support point, a characteristic distance $\hat{d}$ is introduced. For defining such a characteristic distance, assume normalized design variables $p_i \in [0,1]$ and a unit hypercube in the h-dimensional design space filled evenly with $J = n_1^h$ points where $n_1 \geq 2$. In this case, the minimum distance between neighboring points is $\hat{d} = 1/(n_1 - 1) = 1/\left(\sqrt[h]{J} - 1\right)$. On the long term, however, points of the set $S^{(i)}$ will settle down to the Pareto-set which generally has one dimension less than the design space and doesn't range over the full design space.

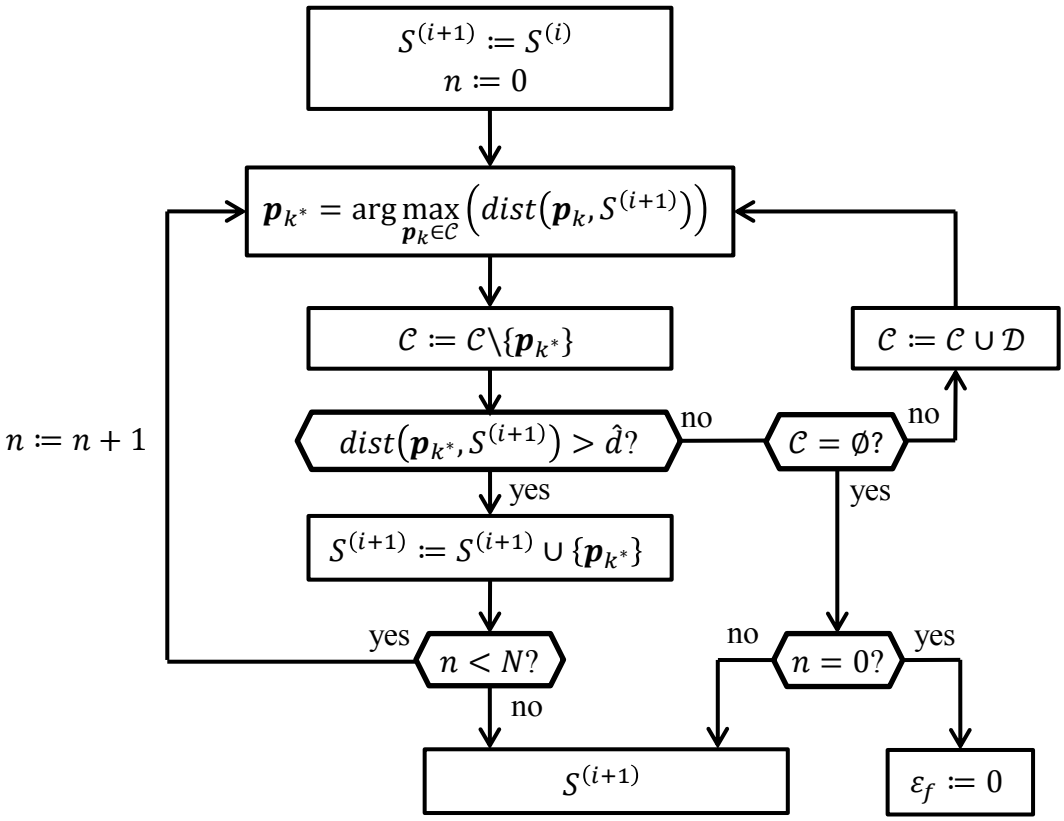

Figure 3: Determination of new support points to update $S^{(i)} \rightarrow S^{(i+1)}$

Thus, h needs to be substituted by $(h-1)$ and the characteristic distance may be defined as

$$\hat{d}\left(J^{(i)}\right) := \frac{a_{\hat{d}}}{\sqrt[h-1]{J^{(i)}} - 1} \tag{7}$$

where $J^{(i)} = \left|S^{(i)}\right|$ is the actual number of support points, and $a_{\hat{d}} > 0$ is a measure of the extent of the Pareto-set to be used as a user-defined tuning factor. If the distance $d(\boldsymbol{p}_{k^*})$ of the potential support point is larger than $\hat{d}$, $\boldsymbol{p}_{k^*}$ is added to the set of support points $S^{(i+1)}$ and the process repeats until a predefined number N of new support points are found. However, if the distance is too small, the set of non-dominated designs $\mathcal{C}$ is extended by the set of dominated designs $\mathcal{D}$, forcing the algorithm to globally update the metamodel. In case that no more sample points are available, meaning $\mathcal{C}$ is empty, only the n support points found so far are used for RS update. However, if no support point could be found at all, i.e., $n = 0$, an error rate ε_f is set to zero and used as convergence criterion as will be discussed later.

After updating the set of support points, original design evaluation is performed for all new support points. Based on the new set $S^{(i+1)}$, response surfaces are built up and the RDO loop in Figure 2 repeats until a maximum number of iterations or a convergence criterion is fulfilled. To check for convergence, approximation quality of the new support points is assessed in the criterion space, meaning that the relative differences between objective values gained from response surfaces $\hat{\boldsymbol{f}}^{RDO}$ and originally evaluated values $\boldsymbol{f}^{RDO}$ are assessed:

$$\varepsilon_f = \max_{l\in\{1\ldots m\},\boldsymbol{p}_k\in S^{(i+1)}\setminus S^{(i)}} \frac{\left|\hat{f}_l^{RDO}(\boldsymbol{p}_k) - f_l^{RDO}(\boldsymbol{p}_k)\right|}{\max\left\{\left|f_l^{RDO}(\boldsymbol{p}_k)\right|, \left|\hat{f}_l^{RDO}(\boldsymbol{p}_k)\right|\right\}} \tag{8}$$

where m is the number of $\boldsymbol{f}^{RDO}$-objectives. If this error rate ε_f is smaller than a predefined error tolerance ε_{tol}, the algorithm is assumed to be converged and the RDO procedure finishes, see Figure 2.

3.2 Test Function

Functionality and efficiency of the proposed process may be proven by using a simple test function. For this purpose, a function [14] is chosen where deterministic and robust optima can be easily recognized and which can be evaluated rather quickly. The problem formulation is similar to Equation (1) where

$$f(\boldsymbol{p};\boldsymbol{r}) = \sum_{i=1}^{2} f_{simple}(p_i + r_i) \tag{9}$$

and

$$f_{simple}(x) = \begin{cases} \cos\dfrac{x}{2} + 1 & for\ -2\pi \le x < 2\pi, \\ 1.1\cos(x+\pi) + 1.1 & for\quad 2\pi \le x < 4\pi, \\ 0 & otherwise. \end{cases} \tag{10}$$

The stochastic variables r_i are uncorrelated and normally distributed with zero mean and variance $\sigma_i^2 = 0.164$. They are truncated at $\pm 2\sigma_i$. The problem formulation (2), (3) for the

aRS based RDO procedure is then applied as presented above, but with the exception that the mean value is maximized:

$$\begin{bmatrix} \max\limits_{\boldsymbol{p}\in P} \mu_f(\boldsymbol{p}) \\ \min\limits_{\boldsymbol{p}\in P} \sigma_f(\boldsymbol{p}) \end{bmatrix} s.t.\ P = \{\boldsymbol{p} \in \mathbb{R}^2 | -2\pi \leq p_i \leq 4\pi\}. \tag{11}$$

A visualization of equation (9) is shown in Figure 4 for $r_i \equiv 0$.

For solving problem (11), firstly the direct integrated RDO procedure shown in Figure 1b is applied. For each design point $\boldsymbol{p}_j$ the robustness evaluation is performed with 20 sample points $\boldsymbol{r}$. The SPEA2 algorithm converges after 2010 design evaluations $\boldsymbol{p}_j$ with a total of $2010 \times 20 = 40200$ function calls resulting in Pareto optimal designs highlighted as white circles in Figure 5a. Obviously there are three non-dominated Pareto optimal designs. The design with the best mean value (upper right white circle) has the worst variance and can easily be identified in Figure 4 as the global maximizer $\boldsymbol{p} = [3\pi, 3\pi]^T$ which has the largest change of slopes in the neighborhood resulting in a high variance. On the contrary, the design with the best variance (lower left white circle) may be identified as local maximizer $\boldsymbol{p} = \boldsymbol{0}$ with the lowest change of slopes in the surrounding, whereas the intermediate solution belongs to one of the two other local maximizers $\boldsymbol{p} = [3\pi, 0]^T$ or $\boldsymbol{p} = [0,3\pi]^T$ in Figure 4.

The same problem is then solved via the RDO process using adaptive RSM. The optimization now requires only 180 designs $\boldsymbol{p}_j$ as support points for the metamodel with a total of $180 \times 20 = 3600$ direct function calls, which is an increase of efficiency of 91%. An anthill plot of the performed RDO can be seen in Figure 5b where support points for the RS are visualized

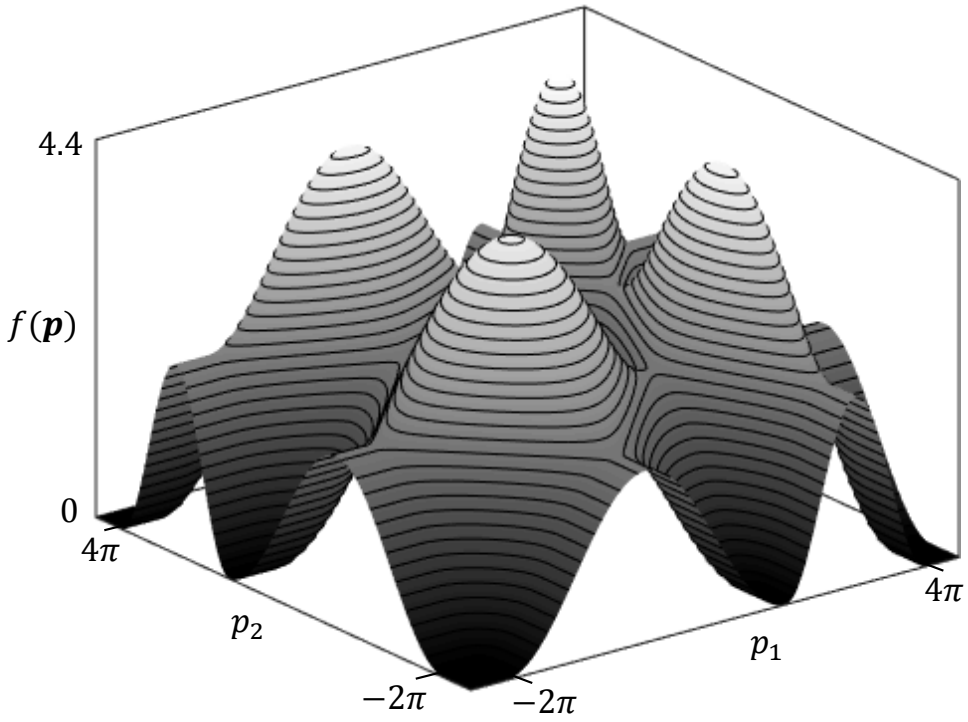

Figure 4: Visualization of the test function (9) for $\boldsymbol{r} = \boldsymbol{0}$

as black dots and all designs used by SPEA2 and computed with the RS are shown as grey dots. Obviously the same important regions are explored resulting in the white circles representing Pareto-optimal designs. Only small deviations in the variance occur, which may be explained by the small sample size for $\boldsymbol{r}$ used for determining mean value and variance. The area which is of no interest shows a poor occurrence of black dots compared to Figure 5a. This is due to the proposed aRSM procedure where usually only intermediate Pareto-optimal designs are chosen as new support points. Hence, the increase of approximation quality of the RS focuses on these areas, whereas unimportant regions are not updated too often.

4 Application to Suspension Design

After successful demonstration, the proposed method may now be applied to robust design of a suspension of a full vehicle model. The vehicle, a luxury passenger car, is modeled as a multibody system (MBS) with 112 rigid bodies and 111 degrees of freedom (DOF). Model components are suspension links, wheel carriers, bushings, spherical joints, springs and dampers, wheels and tires, a steering system, a subframe at the rear axle and the main body, leading to a complex model with a huge number of DOFs as mentioned above. Two different comfort oriented loadcases are investigated, which will be explained later. The main goal is to find a bushing setup which has the best robust performance w.r.t. to the specific objectives and uncertainties. The uncertainties shall emulate different car derivatives which have the same track width, wheelbase and kinematic hardpoints, but different mass and size.

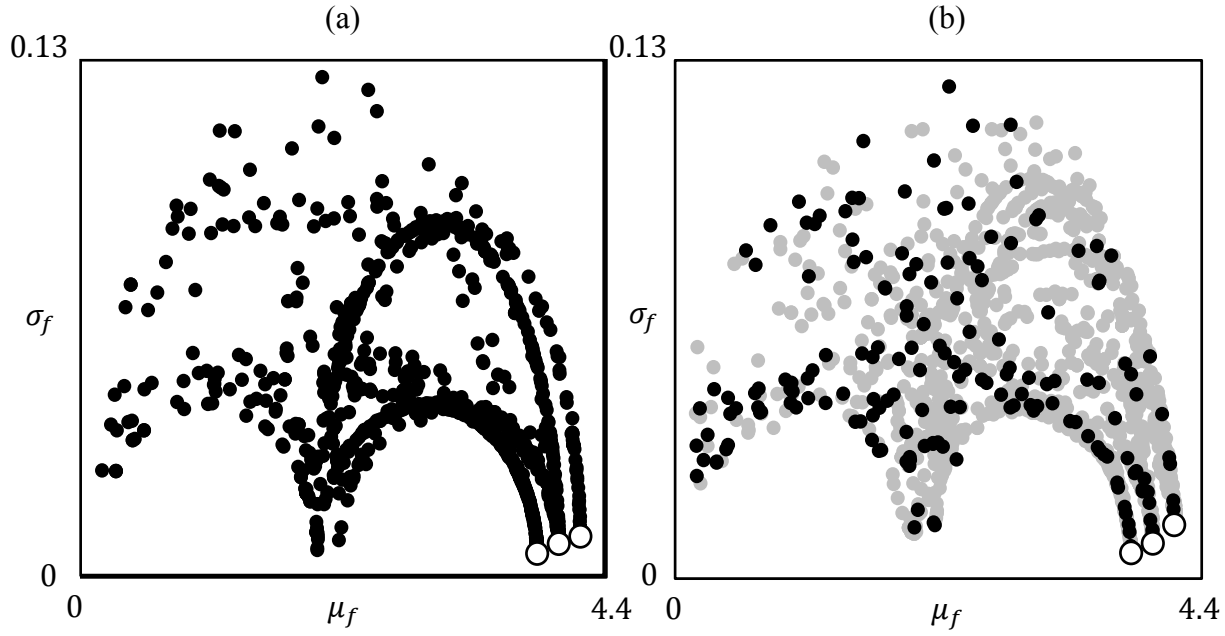

Figure 5: Evaluated designs in criterion space obtained with direct evaluation (a) and aRSM approach (b)

4.1 Design Goals

Design goals are to minimize the oscillation intensities of two typical driving maneuvers. The first loadcase is called axle tramp which is a coupled oscillation between wheel and axle appearing while a car is accelerating or braking. In this paper only axle tramp during braking is investigated. Depending on axle kinematics, the wheel moves backwards and upwards due to the applied braking force F_B, which leads to a loss of road contact F_{WL} and thus reduces the friction force on the tire. This, however, lets the wheel swing back gaining more road contact again. Repetition results in the oscillation illustrated in Figure 6. The most sensitive parameters for this scenario are tire mass and stiffness as well as bushing stiffness and damping where a certain amount of damping should be realized in particular.

To get a reproducible axle tramp behavior in the simulation, an initial vertical force impulse is applied to the rear wheels while the car is braking. The resulting longitudinal and vertical accelerations of the rear wheels in time-domain are squared, integrated and chosen as characteristic responses to be minimized. In order to overcome the misleading influence of the steady acceleration due to braking, the mean longitudinal acceleration of each wheel is subtracted in criteria f_1 and f_2:

$$f_1 = \int \left(\ddot{x}_{W,r} - \bar{\ddot{x}}_{W,r}\right)^2 dt\,, \qquad f_2 = \int \left(\ddot{x}_{W,l} - \bar{\ddot{x}}_{W,l}\right)^2 dt,$$
$$f_3 = \int \ddot{z}_{W,r}{}^2 dt\,, \qquad f_4 = \int \ddot{z}_{W,l}{}^2 dt. \tag{12}$$

In the second loadcase the vehicle is driving with constant speed on a straight road while a single step-shaped roadway excitation occurs at the rear axle. Here, the acceleration of the driver's seat in opposite driving direction is investigated in time-domain and should be minimized. Especially the first acceleration peak can be recognized by passengers and

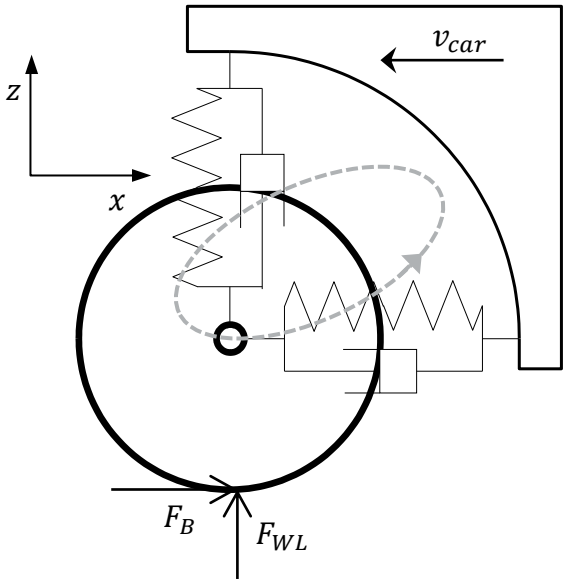

Figure 6: Schematic tire movement during tramp oscillation

therefore is of particular interest. The response is calculated similar to the others shown above:

$$f_5 = \int \ddot{x}_S{}^2 dt. \tag{13}$$

To minimize the seat acceleration in x-direction, the axles should provide enough longitudinal compliance and little damping.

For each of these response criteria mean value and variance are calculated as presented in Section 3.1, normalized w.r.t. a reference car, and partly summed up to finally achieve two objectives for each loadcase:

$$\begin{aligned} \mu_1 &= \sum_{i=1}^{4} \frac{\mu_{f_i}}{\mu_{f_i,ref}}, \qquad \sigma_1 = \sum_{i=1}^{4} \frac{\sigma_{f_i}}{\sigma_{f_{i,ref}}}, \\ \mu_2 &= \frac{\mu_{f_5}}{\mu_{f_5,ref}}, \qquad \sigma_2 = \frac{\sigma_{f_5}}{\sigma_{f_{5,ref}}}. \end{aligned} \tag{14}$$

The different needs of both loadcases regarding stiffness and damping should lead to compromised bushing setups forming a Pareto-front. These tradeoffs are hard to find by human search which is why the proposed computer based optimization procedure will be used.

4.2 Design Parameters

The stiffness and damping characteristics of the suspension bushings are chosen as design parameters, where the bushings are represented by a Kelvin-Voigt (KV) model as shown in Figure 6. This model is rather limited in terms of approximating real bushing behavior, but it needs only two parameters which is rather efficient. The main drawback is that it is not able to reproduce the amplitude and frequency dependency of rubber material used for vehicle bushings [15]. Figure 7 shows the frequency dependent behavior $G(i\omega)$ of a measured real bushing in comparison to the KV model where $c_{dyn} = |G(i\omega)|$ and $\varphi = \sphericalangle G(i\omega)$. To overcome this lack of approximation quality, the KV model is parametrized to match the real bushing behavior only for a specific excitation frequency $f_e \in [0, \tilde{f}]$. This is possible since the two considered loadcases, i.e., axle tramp and free vibration after obstacle crossing, have well defined excitation frequencies f_e, respectively.

Let $c_{dyn}^{ref}(f_e)$ and $\varphi^{ref}(f_e)$ be the dynamic stiffness and loss angle of a reference bushing obtained from measurements, see Figure 7. Then the characteristic of c_{dyn}^{ref} for different excitation frequencies f_e can be expressed by a factor $k_c(f_e) = c_{dyn}^{ref}(f_e)/c^{ref}$ representing the amount of dynamic hardening w.r.t. static stiffness $c^{ref} \coloneqq c_{dyn}^{ref}(0)$. For the actual car design, only the static stiffness of the bushing $c^* \coloneqq c_{dyn}(0)$ is changed as design variable, whereas the hardening characteristic is kept constant. Then the dynamic stiffness for a given excitation frequency may be calculated as $c_{dyn}(f_e) = c^* k_c(f_e)$. Since the frequency dependence of the loss angle $\varphi^{ref}(f_e)$ is small compared to the change in dynamic stiffness,

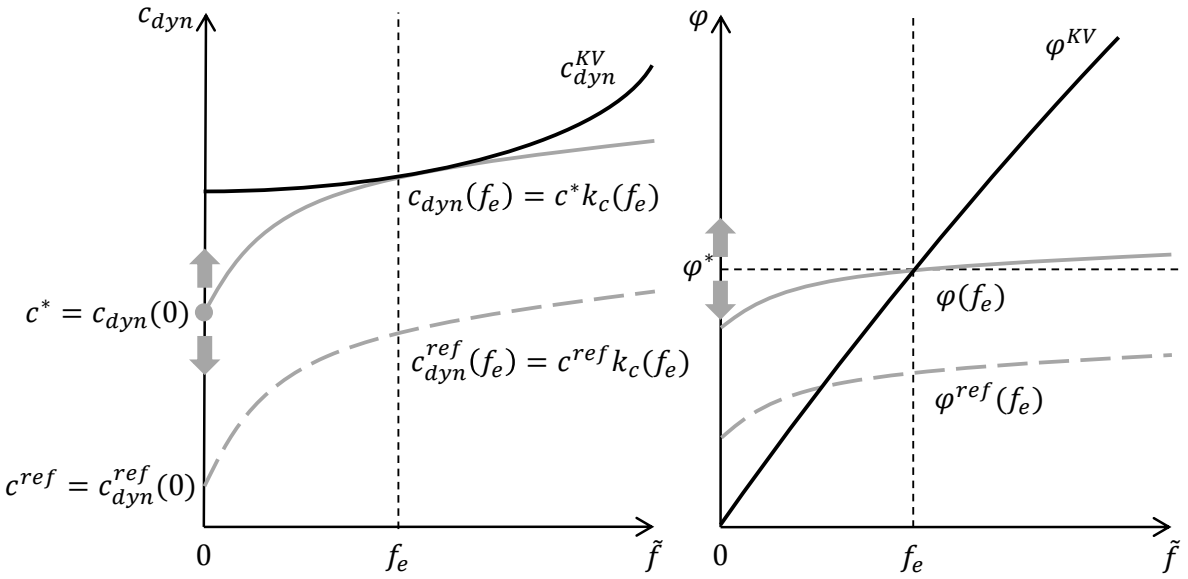

Figure 7: Comparison of Kelvin-Voigt model (black) and real bushing behavior (grey)

see Figure 7, it is assumed to be independent of f_e for this optimization. Thus, the actual design parameter φ^* is used for all frequencies, i.e., $\varphi(f_e) \approx \varphi^*$. For simulation of axle tramp and obstacle crossing, the actual frequencies f_e are identified and the corresponding values $c_{dyn}(f_e)$ and $\varphi(f_e)$ are computed form the bushing design variables c^*, φ^* and the hardening characteristic $k_c(f_e)$. Then these values are converted to corresponding values of stiffness c and damping d of KV model force

$$F(t) = cx(t) + d\dot{x}(t). \tag{15}$$

In order to find proper transformation equations, we firstly apply Laplace-Transformation $F(s) = \mathcal{L}\{F(t)\}$ to Equation (15) where $s = i\omega = i2\pi f_e$. This results in the transfer function

$$G(i\omega) = \frac{F(i\omega)}{x(i\omega)} = c + id\omega \tag{16}$$

of the KV model. Dynamic stiffness c_{dyn} and loss angle φ of the KV model are then defined as

$$c_{dyn}^{KV}(\omega) = |G(i\omega)| = \sqrt{c^2 + d^2\omega^2}, \qquad \varphi^{KV}(\omega) = \sphericalangle G(i\omega) = \arctan\left(\frac{d\omega}{c}\right). \tag{17}$$

Inverting these two equations for given c_{dyn} and φ finally results in equivalent values for c and d used in the KV model matching the real bushing behavior at the specified excitation frequency:

$$c = c_{dyn}\cos\varphi = c^* k_c(f_e) cos\varphi^*, \qquad d = \frac{c_{dyn}\sin\varphi}{2\pi f_e} = \frac{c^* k_c(f_e) sin\varphi^*}{2\pi f_e}. \tag{18}$$

In total the vehicle model has 10 bushings, where here only translational bushing characteristics are changed. Therefore, 60 parameters, precisely c^* and φ^* for each coordinate direction of each bushing, may be considered. To minimize the amount of design parameters, a sensitivity analysis was performed resulting in only 11 important parameters summarized in design vector

$$\boldsymbol{p} = \underbrace{\left[c_{1,x}^*, \varphi_{1,x}^*, c_{1,z}^*, \varphi_{1,z}^*, \varphi_{2,x}^*, \varphi_{3,x}^*, c_{3,z}^*, \varphi_{3,z}^*, \varphi_{4,x}^*, c_{4,z}^*, \varphi_{4,z}^*\right]^T}_{\begin{matrix} K1 & K2 & K3 & K4 \end{matrix}}. \tag{19}$$

The associated bushings and their individual coordinate systems $K1$ to $K4$ are visualized in Figure 8. Loss angle values φ^* are varied between 1° and 10° and static stiffness values c^* between $0.8c^{ref}$ and $1.2c^{ref}$ resulting in bounds

$$\begin{aligned} \boldsymbol{p}_l &= \left[0.8c_{1,x}^{ref}, 1°, 0.8c_{1,z}^{ref}, 1°, 1°, 1°, 0.8c_{3,z}^{ref}, 1°, 1°, 0.8c_{4,z}^{ref}, 1°\right]^T, \\ \boldsymbol{p}_u &= \left[1.2c_{1,x}^{ref}, 10°, 1.2c_{1,z}^{ref}, 10°, 10°, 10°, 1.2c_{3,z}^{ref}, 10°, 10°, 1.2c_{4,z}^{ref}, 10°\right]^{\mathrm{T}}. \end{aligned} \tag{20}$$

The optimization is performed using normalized design variables

$$p_i^* = \frac{p_i - p_{i,l}}{p_{i,u} - p_{i,l}} \in [0,1], \qquad i = 1, \dots, 11. \tag{21}$$

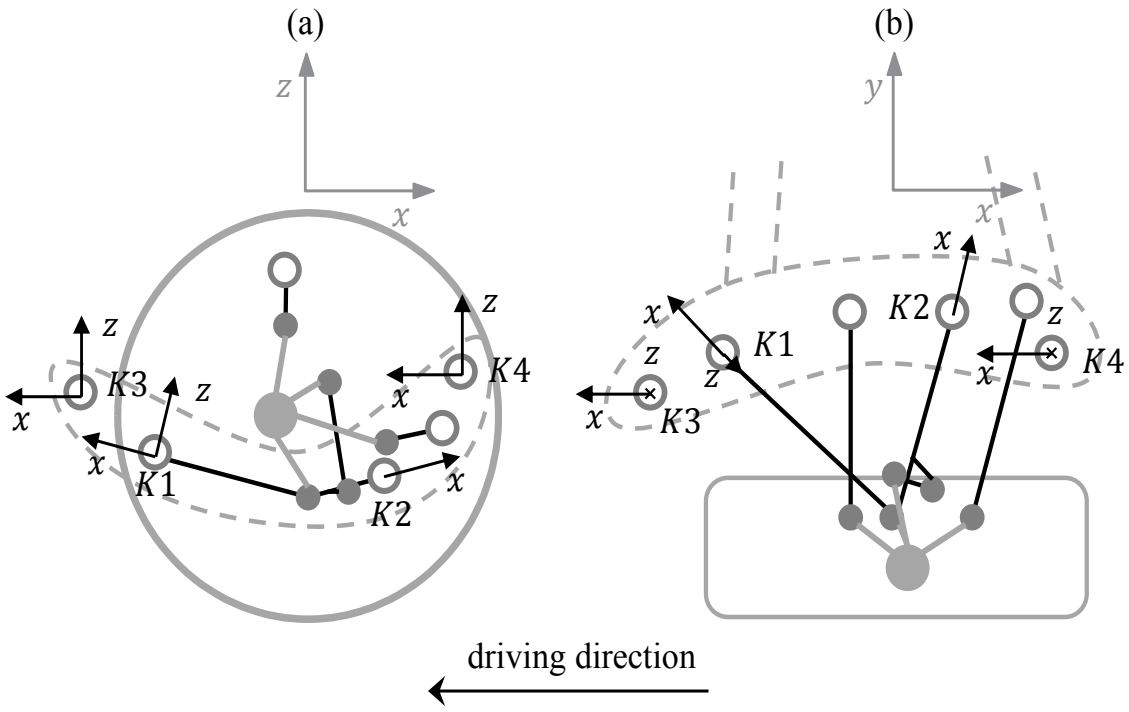

Figure 8: Side (a) and top view (b) of investigated rear axle with wheel carrier (grey), linkages (black), bushings (white circles) and subframe (gray dashed)

4.3 Uncertainties

A passenger car underlies several uncertainties. In this paper scatter of mass properties of loading and bodies is investigated. More precisely, variation of passenger numbers, fuel level, boot loading, extra equipment, engine and battery type are taken into account where positions are assumed to be given according to Figure 9. All these variations lead to a change of masses summarized in an uncertainty vector

$$\boldsymbol{r} \coloneqq \left[m_{P1}, m_{P2}, m_{P3}, m_{P4}, m_E, m_F, m_T, m_B, m_{EQ}\right]^T \tag{22}$$

where m_{P1} to m_{P4} refer to passenger masses, m_E to the engine mass, m_F to the fuel mass, m_T to the trunk mass, m_B to the battery mass, and m_{EQ} to mass of extra equipment. The uncertainty vector $\boldsymbol{r}$ is varied between the following bounds:

$$\boldsymbol{r}_l = [40,0,0,0,130,0,0,0,0]^T, \qquad \boldsymbol{r}_u = [100,100,100,100,215,70,50,115,170]^{\mathrm{T}}. \tag{23}$$

Mass variations have direct influence on mass properties of the car body, namely overall mass m_{CB} center of gravity (CG) position $\boldsymbol{s}_{CB}$ and inertia tensor $\boldsymbol{I}_{CB}$, which can be calculated w.r.t. the overall CG using the parallel axes theorem [16].

Due to lack of statistics for the masses described above, they are assumed to be normally distributed and independent. For sampling purpose, a truncated standard normal distribution $z_i \sim N(0,1)$ is used for each parameter and generated with the aLHS method mentioned above. The distribution is truncated to $z_i \in [-2,2]$ in order to suspend infinite values and normalized to $0 \leq z_i^* \leq 1$ by

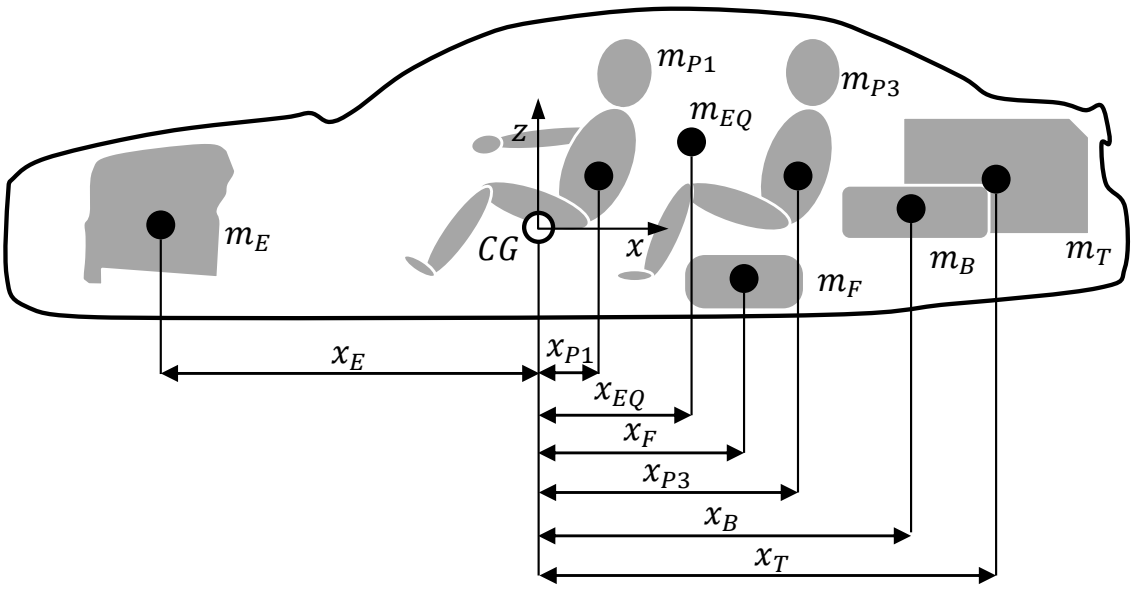

Figure 9: Uncertain masses

$$z_i^* := \frac{2 + z_i}{4}. \tag{24}$$

Finally, the parameters with specific ranges (23) and units used in the model can be calculated via

$$r_i = r_{i,l} + z_i^*(r_{i,u} - r_{i,l}) \,, \qquad i = 1, \dots, 9. \tag{25}$$

4.4 Optimization Results

The RDO is performed subject to design objectives (14), normalized design parameters (21) and uncertainties (25). For evaluation of robustness measures, a sample size of 20 is used for uncertainties. The initial set $S^{(0)}$ contains 30 support points. In each iteration $N = 5$ new support points are added to improve the RS. The SPEA2 performs optimization on the RS with a maximum of 150 generations with 20 new individuals in each generation. The RDO procedure is limited to 40 adaptions of the RS resulting in a maximum of $30 + 40 \times 5 = 230$ original design evaluations. While running 10 simulations in parallel, the overall RDO took 6 days and 9 hours until it converged after already 38 adaption iterations. The evaluated support points are shown in Figure 10. It is clearly visible, that all criteria are improving simultaneously resulting in a rather narrow Pareto-front indicating that the mean objectives are not as contradicting as assumed. Nevertheless, both criteria could be improved w.r.t. the reference vehicle setup where also robustness seems to be improved. For better visualization of the improvement, histograms of two specific objectives of a Pareto-optimal design $\mathcal{O}$ lying on the knee of the front are shown in Figure 12 and compared to the reference set up. It can be easily observed that mean value and variance of f_2 defined in Equation (13) are both

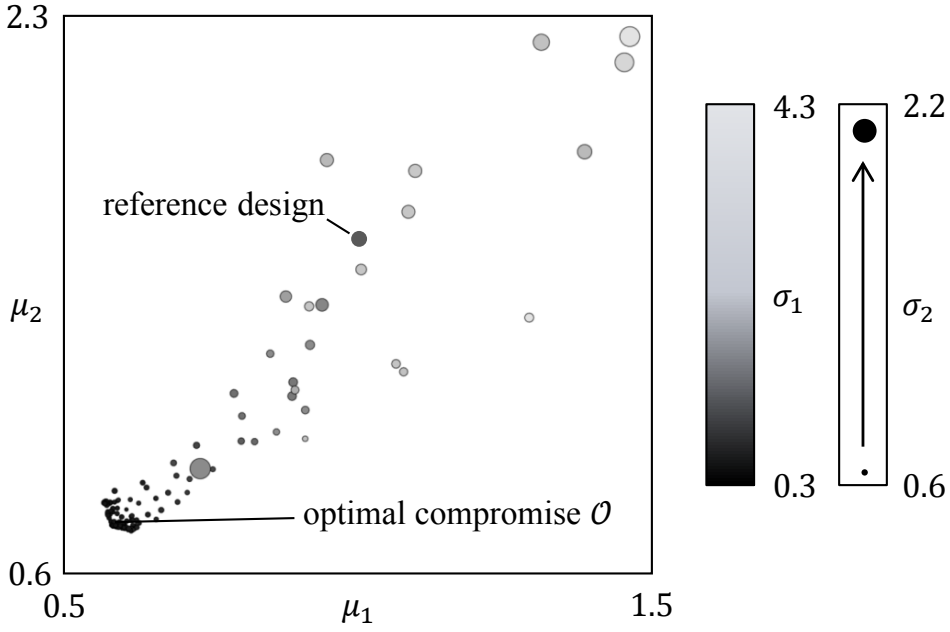

Figure 10: 4D-Pareto plot of support points

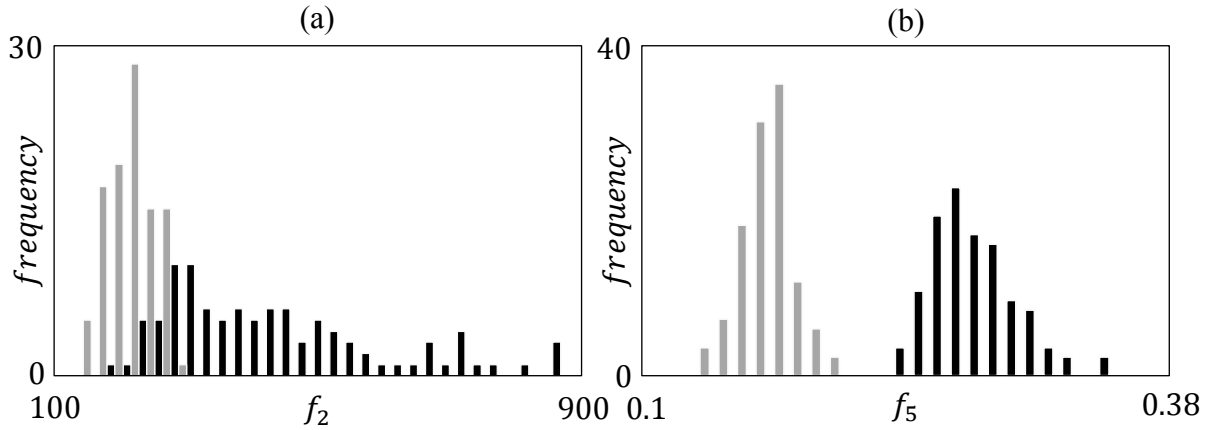

Figure 12: Frequency plot of objectives f_2 (a) and f_5 (b) for optimal compromise design $\mathcal{O}$ (grey) and reference design (black)

significantly improved. The same is true for the mean value of f_5 defined in Equation (13), whereas the scatter of f_5 is only slightly improved. The corresponding accelerations determining f_2 and f_5, namely the acceleration of the left tire (Figure 11a) and the driver's seat (Figure 11b) in x-direction confirm the histogram information in Figure 12 in the time-domain. Especially the large scatter in tire oscillation of the reference car during axle tramp can be observed.

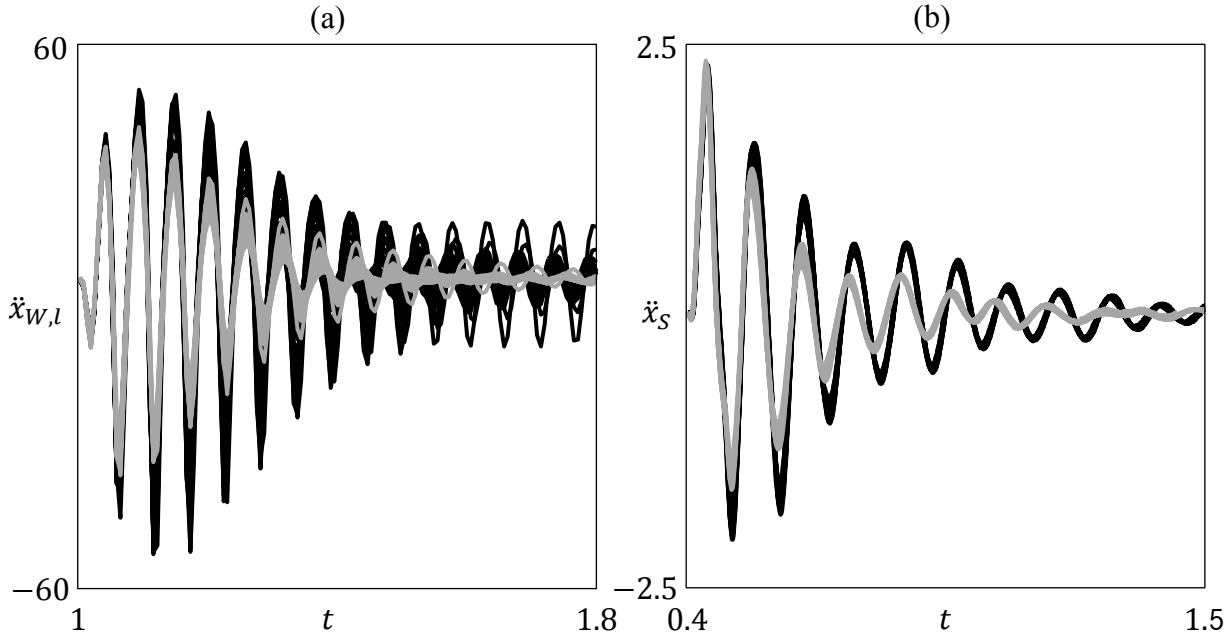

Figure 11: Time plots of tire acceleration during tramp oscillation (a) and driver's seat acceleration after obstacle crossing (b) acceleration of optimal design $\mathcal{O}$ (grey) and reference design (black)

5 Conclusions

The paper demonstrates an efficient multi-objective robust design optimization procedure. Implementation of an adaptive response surface modeling strategy significantly reduces computational effort compared to direct optimization which is proven by optimizing a simple test function. An application of the proposed method to vehicle suspension design by using multibody system simulations and optiSLang is successfully performed. Optimization is done in terms of minimizing predefined accelerations measured throughout the loadcases axle tramp and single step-shaped roadway excitation for a given range of bushing stiffnesses and damping parameters under presence of scattering vehicle masses. Although both loadcases need contrary bushing characteristics, optimal compromise designs could be found where mean value and variance of the vehicles dynamical behavior are significantly improved compared to a reference design.

6 References

[1] Most, T. and Will, J., "Robust Design Optimization in Industrial Virtual Product Development," Weimar, Germany, http://www.dynardo.de/fileadmin/Material_Dynardo/bibliothek/RDO/MOST_2012_REC_RobustDesignOptimizationInIndustrialVirtualProdctDevelopment.pdf, January 13, 2015.

[2] Cheng, X. and Lin, Y., "Multiobjective Robust Design of the Double Wishbone Suspension System Based on Particle Swarm Optimization," *The Scientific World Journal*, 2014, doi:10.1155/2014/354857.

[3] Kang, D.O., Heo, S.J., Kim, M.S., Choi, W.C. et al., "Robust Design Optimization of Suspension System by Using Target Cascading Method," *International Journal of Automotive Technology* 13(1):109–122, 2011, doi:10.1007/s12239−012−0010−y.

[4] Park, K., Heo, S.J., Kang, D.O., Jeong, J.I. et al., "Robust Design Optimization of Suspension System Considering Steering Pull Reduction," *International Journal of Automotive Technology* 14(6):927–933, 2013, doi:10.1007/s12239−013−0102−3.

[5] Yang, Q., Huang, J., Wang, G., and Karimi, H.R., "An Adaptive Metamodel-Based Optimization Approach for Vehicle Suspension System Design," *Mathematical Problems in Engineering* 2014:1–10, 2014, doi:10.1155/2014/965157.

[6] Busch, J. and Bestle, D., "Optimisation of Lateral Car Dynamics Taking Into Account Parameter Uncertainties," *Vehicle System Dynamics* 52(2):166–185, 2014, doi:10.1080/00423114.2013.868006.

[7] DYNARDO - Dynamic Software and Engineering GmbH, "optiSLang - Software für Sensitivitätsanalyse, Mehrzieloptimierung, multidisziplinäre Optimierung, Robustheitsbewertung, Zuverlässigkeitsanalyse und Robust Design Optimierung," http://www.dynardo.de/software/optislang.html, April 21, 2015.

[8] Bucher, C., "Using Response Surface Methodology for Robust Design Optimization: Introduction and Overview," 4th Weimar Optimization and Stochastic Days 29/30, 2007.

[9] Schneider, D. and Bucher, C., “Efficient RDO Using Sample Recycling,” Weimar Optimization and Stochastic Days 5.0, 2008.

[10] Huntington, D.E. and Lyrintzis, C.S., “Improvements to and Limitations of Latin Hypercube Sampling,” *Probabilistic Engineering Mechanics* 13(4):245–253, 1998, doi:10.1016/S0266-8920(97)00013-1.

[11] Will, J. and Most, T., “Metamodell of Optimal Prognosis (MOP) - an Automatic Approach for User Friendly Parameter Optimization,” 6th Weimar Optimization and Stochastic Days, Weimar, Germany, http://www.dynardo.de/fileadmin/Material_Dynardo/bibliothek/WOST_6.0/WOST_6_Paper_Will_Most.pdf, January 13, 2015.

[12] DYNARDO - Dynamic Software and Engineering GmbH, “Recent Developments in the Metamodel of Optimal Prognosis,” 11th Weimarer Optimization and Stochastic Days, Weimar, Germany, http://www.dynardo.de/fileadmin/Material_Dynardo/bibliothek/WOST11/11_WOST2014_Session3_Most.pdf, January 13, 2015.

[13] Zitzler, E., Laumanns, M., and Thiele, L., “SPEA2: Improving the Strength Pareto Evolutionary Algorithm,” TIK-Report 103, 2001.

[14] Vis, J.K., “Particle Swarm Optimizer for Finding Robust Optima,” Leiden, The Netherlands, http://www.liacs.nl/assets/Bachelorscripties/2009-12JonathanVis.pdf, January 15, 2015.

[15] Pfeffer, P. and Hofer, K., “Einfaches nichtlineares Modell für Elastomer- und Hydrolager,” *ATZ* 104(5):442–446 and 450-451, 2002.

[16] Woernle, C., “Mehrkörpersysteme: Eine Einführung in die Kinematik und Dynamik von Systemen starrer Körper,” Springer, Berlin, 2011.